Engineering Structures 295 (2023) 116800

Contents lists available at ScienceDirect

Engineering Structures

journal homepage: www.elsevier.com/locate/engstruct

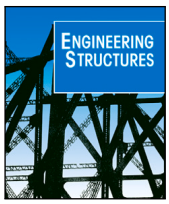

Load introduction to composite columns revisited—Significance of force allocation and shear connection stiffness

B. Grzeszykowski [a,*], M.J. Lewandowski-Szewczyk [b], M. Niedośpiał [a]

[a] Faculty of Civil Engineering, Warsaw University of Technology, al. Armii Ludowej 16, 00-637 Warsaw, Poland
[b] Faculty of Civil and Environmental Engineering, Gdańsk University of Technology, Narutowicza 11/12, 80-233 Gdańsk, Poland

ARTICLE INFO

Keywords:
Composite column
Shear transfer
Load introduction
Shear stiffness
Shear connection
Force allocation

ABSTRACT

The AISC 360-16 Specification recommends that the design shear force between parts of a composite column in the load introduction area shall be calculated based on the force allocation at ultimate limit state. Applicability of this straightforward method to the load levels that usually arise in slender composite columns is questionable, as this capacity-based force allocation is only true when the axial force is equal to the plastic resistance of the composite cross-section. Next, the number of required shear connectors is calculated as a quotient of the design shear force and the strength of a single shear connector. We demonstrate that: first, for the lower load levels, the stiffness-based force allocation gives a more accurate estimate of the shear force; second, the number of shear connectors satisfying the strength requirement can lead to insufficient force transfer between parts of the composite cross-section. To investigate the shear transfer mechanism in composite columns, we derive an analytical model with linear elastic constitutive relations both for steel and concrete and three types of shear force slip laws: elastic, elastic plastic, and rigid plastic. The case studies carried out for different shear transfer scenarios demonstrate the importance of the shear connection stiffness on the effectiveness of the load introduction. The remaining portion of the shear force is transferred outside the load introduction area, which hampers the column's ability to withstand shearing from varying bending moments or incipient buckling. To control the shear force transfer efficiency by enhancing the shear connection stiffness, we propose an original Stiffness Method and provide design charts as an aid in the design process.

1. Introduction

In current editions of design guides in Europe [1] and the USA [2], the capacity of the shear connection is the central concern in designing shear transfer in composite columns. The shearing between the concrete and steel arises due to the column bending as a result of transverse loading or unequal end moments, and when the axial load is introduced to the column through one of the materials. In the latter case, the role of the shear connection is to transfer the relative portion of the axial load to the other components of the composite cross-section. The question arises if the shear connection stiffness impacts the effectiveness of the transferring mechanism at much lower load levels than the design resistance of the composite cross-section. In current editions of design guides in Europe [1] and the USA [2], this problem is unaddressed. As we will show in this paper, through analytical solutions of the axially loaded composite columns with corresponding shear transfer models, the effectiveness of the load transfer depends heavily on the stiffness of the shear connection in the load introduction area.

The second issue concerns establishing the force to be transferred between the materials. AISC [2] recommends calculating the shearing force proportional to the plastic capacity of the part of the cross-section to which the axial load is to be transferred. In the case of concrete-filled composite members with slender cross-sections, which are prone to local buckling, loaded through the concrete, the yield stress of the steel portion should be reduced to the critical buckling stress of the steel cross-section. This means that the design shear force is always related to the axial force ratio in the ultimate limit state of the composite cross-section driven by yield or local buckling critical stress. However, before the yielding of the steel and for stress levels in concrete for which the behavior is almost linear, the axial load is distributed proportionally to the axial stiffness of the composite member components [3]. The European standard [1] addresses this issue as it recommends taking maximum shear force from the elastic or plastic theory, cf. [clause 6.7.4.2(1) in 1] and Johnson [4]. In the spectrum between the stiffness-based and capacity-based solutions, the nonlinearity of the concrete and

* Corresponding author.
E-mail addresses: bartosz.grzeszykowski@pw.edu.pl (B. Grzeszykowski), maciej.szewczyk@pg.edu.pl (M.J. Lewandowski-Szewczyk), marcin.niedospial@pw.edu.pl (M. Niedośpiał).

https://doi.org/10.1016/j.engstruct.2023.116800
Received 22 March 2023; Received in revised form 7 July 2023; Accepted 21 August 2023

the yielding of steel should be considered. We will investigate the force distribution in the composite cross-section components with the aid of material models according to European standards [5,6].

The vast majority of the previous research has been focused on push-out tests evaluating the strength and stiffness of the shear connection utilizing shear studs, e.g., [7–9] or bond strength for various composite cross-sections [10–13]. The problem of force transfer from one material to another in columns obtained significantly smaller attention in the research community. The most notable contributions are those of Dunberry et al. [14] and Wium and Lebet [3], however both considered only bond interaction.

Dunberry et al. [14] have considered load transfer in preloaded concrete-filled tubes when the additional load is introduced through shear tabs welded directly to the tube. However, the authors presented forces in concrete and steel only for loads very close to the ultimate load, where the force allocation according to plastic contributions is applicable. Interestingly, the authors established the load transfer area as not exceeding two times the minimum transverse direction of the composite cross-section both above and below the force introduction in the ultimate limit state, which is recommended by the AISC Specification [2]. The European standard [1] is more conservative as it limits the load transfer length to two times the minimum transverse direction or a third of the column's length, whichever gives a smaller transfer length. Mollazadeh and Wang [15] built a numerical model of the aforementioned experiment and obtained very good agreement between the FE results and experiments. However, again the focus of the paper was on load introduction at the ultimate cross-section capacity load level. Next, the authors considered a setting where the whole load is applied through the shear tab connections at the same height, which resulted in the local buckling of the steel tube just below the shear plates. In a follow-up study, Mollazadeh and Wang [16] performed a series of experiments on relatively short columns with and without shear studs below the shear plates. The shear studs significantly improved the force transfer from steel to concrete, but the composite action is not achieved at a distance two times the composite cross-section dimension below the shear tabs connection as strains in the concrete core and steel tube differ [Fig. 18(c-d) in 16]. This observation prompted us to examine closely the parameters influencing the effectiveness of load transfer.

In a study investigating the bond behavior of short composite columns loaded through steel and consisting of a wide flange I-section encased in concrete, Wium and Lebet [3] have considered the influence of chosen parameters on chemical bond strength and maximum shear stress on the concrete-steel interface after debonding. It is worth noting that it is one of the very few papers that deal with short columns in examining the bond behavior and, more importantly, the authors analyze the force distribution at load levels below the ultimate load. Wium and Lebet [3] argue that such an allocation should be proportional to the axial stiffness of the composite member parts, and not to the relative cross-sectional strength contributions. As stated above, the exact force distribution for axial force levels between the onset of loading and the ultimate load has to consider concrete nonlinearity and the yielding of steel. Furthermore, Wium and Lebet [3] report that in the previous study of Wium [17], the author established the bond modulus between the steel and concrete prior to debonding as $500\,\mathrm{N/mm^3}$. However, there is no consensus in the literature if the bond modulus is a real interface property or if it serves as a model parameter regularizing the rigid plastic or frictional contact model [18]. The approach adopted in the current design guides [1,2,19] leans towards the latter and disregards the stiffness of the bond interface. Similarly, in reinforced concrete structures the interaction between the concrete and rebar modeled with the rigid plastic bond law is considered a rough but sound simplification [20].

The purpose of this study is to explore the relationship between the shear connection stiffness and the effectiveness of the force transferring mechanism for the load levels found in service or the ultimate limit state of columns for which stresses are lower than plastic, i.e., driven by global or local buckling. To achieve this goal, in Section 2, we investigate the axial force distribution in composite cross-sections with the aid of material models allowed by European standards [5,6]. We prove that for a wide range of applications, the nonlinearity of concrete on the onset of the loading path might be neglected in establishing the force distribution. In Section 3, a brief overview of the allowed force transfer mechanisms according to the current design guides [1,2] is given. In Section 4, we present closed-form analytical solutions for a load introduction problem with the elastic, elastic plastic, and rigid plastic shear interface model within and outside of the transfer length. The applicability of the shear transfer models in considered scenarios is discussed. The high point of the research is the introduction of the original Stiffness Method in Section 5 intended to ensure acceptable axial force transfer along the load introduction area. We present design charts for assessing the stiffness of the shear connection to fulfill this requirement. Additionally, we compare results obtained with the EN 1994-1-1 [1] and with the proposed Stiffness Method regarding the force transfer achieved. The design for strength confirms that the force transfer might be unsatisfactory. Finally, in Section 6, we summarize our work and propose to include in the existing design guides the shear demand in the load transfer area.

2. Allocation of sectional forces

To design the load transfer mechanism, first and foremost, one needs to know the portion of the axial force which needs to be conveyed from the loaded component to other parts of the composite cross-section. The ratio of the axial force carried by the composite cross-section components to the total axial force depends on the considered stress level. At the ultimate load, when all parts of the composite cross-section reach the maximum stress driven by the yield of steel f_{a}, and concrete f_{c}, the capacity-based force allocation of the introduced load N_{Ed} is proportional to the strength contributions of the cross-section's parts [2,14],

$$\begin{aligned} N_{\mathrm{a,cb}} &= \frac{A_{\mathrm{a}} f_{\mathrm{a}}}{N_{\mathrm{pl,Rd}}} N_{\mathrm{Ed}}, \\ N_{\mathrm{c,cb}} &= \left(1 - \frac{A_{\mathrm{a}} f_{\mathrm{a}}}{N_{\mathrm{pl,Rd}}}\right) N_{\mathrm{Ed}}, \end{aligned} \tag{1}$$

where A_{a} denotes the area of the steel part and $N_{\mathrm{pl,Rd}}$ design resistance of the cross-section. Note, that $N_{\mathrm{pl,Rd}}$ factors in reductions of concrete strength for concrete-encased cross-sections ($0.85 f_{\mathrm{c}}$), and local buckling of steel tubes in concrete-filled composites [1,2]. In the latter case, f_{a} in Eq. (1) should be replaced with the critical local buckling stress of the steel tube wall. For the sake of clarity, we will consider the simplest case: concrete without reinforcement and the full yield stress of steel and concrete. Yet, these simplifications do not invalidate the general conclusions drawn from the presented considerations.

On the onset of the loading path, the stiffness-based force allocation holds, which is proportional to the axial stiffness of the composite cross-section constituents [3],

$$\begin{aligned} N_{\mathrm{a,sb}} &= A_{\mathrm{a}} \sigma_{\mathrm{a}} = \frac{\alpha\omega}{1+\alpha\omega} N_{\mathrm{Ed}}, \\ N_{\mathrm{c,sb}} &= A_{\mathrm{c}} \sigma_{\mathrm{c}} = \frac{1}{1+\alpha\omega} N_{\mathrm{Ed}}, \end{aligned} \tag{2}$$

where $\omega = A_{\mathrm{a}}/A_{\mathrm{c}}$, σ_i denotes the axial stress of cross-section part i, and $\alpha = E_{\mathrm{a}}/E_{\mathrm{c}}$ with E_i being Young's modulus. Note that subscripts "a" and "c" refer to the steel and concrete parts of the cross-section throughout this paper.

The European standard [1] recommends taking as a design shear force a maximum difference from the introduced load and the final value resulting from allocation using the stiffness-based (2) and capacity-based (1) approach. For example, for a stress free column loaded through concrete with the load N_{Ed}, the design shear force is $V_{\mathrm{Ed}} = \max(N_{\mathrm{a,sb}}, N_{\mathrm{a,cb}})$. However, as stated before, the stiffness-based

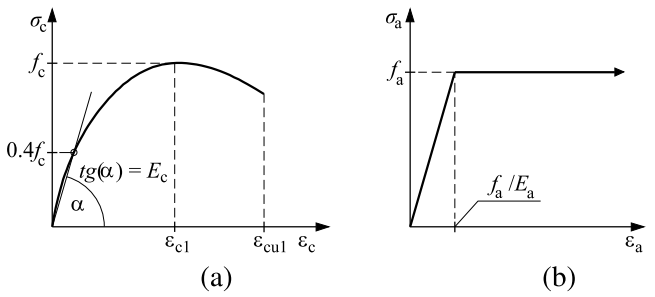

Fig. 1. Stress–strain relation assumed for: (a) concrete and (b) steel.

force allocation is true only on the onset of the loading path, and the capacity-based force allocation holds only for an ultimate axial load. The AISC Specification [2] considers only the capacity-based allocation of forces, which is inadequate for lower load levels.

For slender composite columns, where buckling limits axial loads, or considering service load levels, one deals with axial forces significantly lower than $N_{\mathrm{pl,Rd}}$. In this range of load levels, the nonlinearity of the concrete, the yielding of the steel, and the ratio of the concrete and steel cross-section areas, play their role in a resulting force distribution. Therefore, the actual force distribution for intermediate load levels is not given by Eq. (1) nor Eq. (2). To illustrate the force distribution for any load level, we will adopt one-dimensional idealized stress–strain relationships allowed in European standards [5,6]. For the concrete in compression, in nonlinear analysis, EN 1992-1-1 [5] recommends the following stress–strain relationship (Fig. 1a):

$$\sigma_{\mathrm{c}}\left(\varepsilon_{\mathrm{c}}\right)=f_{\mathrm{c}}\frac{k_{\mathrm{c}}\left(\frac{\varepsilon_{\mathrm{c}}}{\varepsilon_{\mathrm{c1}}}\right)-\left(\frac{\varepsilon_{\mathrm{c}}}{\varepsilon_{\mathrm{c1}}}\right)^{2}}{1+\left(k_{\mathrm{c}}-2\right)\left(\frac{\varepsilon_{\mathrm{c}}}{\varepsilon_{\mathrm{c1}}}\right)} \tag{3}$$

where: $k_{\mathrm{c}}=1.05E_{\mathrm{c}}\varepsilon_{\mathrm{c1}}/f_{\mathrm{c}}$, $\varepsilon_{\mathrm{c1}}=\min(0.7(f_{\mathrm{c0}})^{0.31},2.8)$ in ‰; f_{c} in MPa; ε_{c} current axial strain. In Eq. (3), f_{c} denotes a mean compressive strength of the cylindrical specimen f_{cm}, and E_{c} is a mean secant Young's modulus E_{cm} calculated at $\sigma_{\mathrm{c}}=0.4f_{\mathrm{c}}$. Note that Eq. (3) compressive stress and strain are positive. This is the convention we will adopt only to establish force allocation with nonlinear models in this section.

We emphasize that compressive strength in (3) is significantly higher than the design compressive strength f_{cd}, which is utilized in the design resistance $N_{\mathrm{pl,Rd}}$. The design compressive strength factors in the statistical scatter of the compression tests' results and an additional safety factor in the spirit of the partial factors method in European standards [1] or Load and Resistance Factor Design in AISC 360-16 [2]. However, the concrete behavior is rather described by the mean values, e.g., when comparing experimental results with the resistance calculated according to standards [16,21]. Therefore, in the following analysis we will use axial ultimate load $N_{\mathrm{U}}=f_{\mathrm{c}}A_{\mathrm{c}}+f_{\mathrm{a}}A_{\mathrm{a}}$ as a reference load in a nonlinear analysis of the composite cross-section. Note that numerous other models have been proposed to describe unconfined [22,23] and confined concrete behavior [24,25], which will not be pursued in this paper.

The advantage of the stress–strain relation (3) is that it is a nonlinear elastic relation that mimics a complicated nonlinear elastic plastic relation with damage in monotonic loading conditions. Thus, one can invert the relation (3) for strains up to $\varepsilon_{\mathrm{c1}}$,

$$\varepsilon_{\mathrm{c}}=\frac{1}{2}\left[k_{\mathrm{c}}\varepsilon_{\mathrm{c1}}+(2-k_{\mathrm{c}})\varepsilon_{\mathrm{c1}}\frac{\sigma_{\mathrm{c}}}{f_{\mathrm{c}}}-\sqrt{\varepsilon_{\mathrm{c1}}^{2}\left(1-\frac{\sigma_{\mathrm{c}}}{f_{\mathrm{c}}}\right)\left(k_{\mathrm{c}}^{2}-(k-2)^{2}\frac{\sigma_{\mathrm{c}}}{f_{\mathrm{c}}}\right)}\right]$$
$$\text{for}\quad \sigma_{\mathrm{c}}\le f_{\mathrm{c}}. \tag{4}$$

For steel, we assume the standard elastic plastic constitutive relationship without hardening [6] (Fig. 1b).

The final values of the stress in steel and concrete after the desired load transfer can be derived considering the composite action, thus, $\varepsilon_{\mathrm{a}}=\varepsilon_{\mathrm{c}}$, and $\sigma_{\mathrm{a}}A_{\mathrm{a}}+\sigma_{\mathrm{c}}A_{\mathrm{c}}=N_{\mathrm{Ed}}$. Typically, the steel yields before the concrete stress reaches f_{c} as the yield strain of steel $f_{\mathrm{a}}/E_{\mathrm{a}}<\varepsilon_{\mathrm{c1}}$ for all grades of concrete and steel up to S355 included. Only for the combination of very weak concrete (≤C25/30) and high strength steel (≥S460) the converse situation arises. After yielding of steel the excessive axial load is carried out solely by the concrete portion of the cross-section and the equilibrium takes the form $f_{\mathrm{a}}A_{\mathrm{a}}+\sigma_{\mathrm{c}}A_{\mathrm{c}}=N_{\mathrm{Ed}}$. Solving this system of equations leads to stresses in steel and concrete for a given load level $n=N_{\mathrm{Ed}}/N_{\mathrm{U}}$,

$$\sigma_{\mathrm{a}}=\begin{cases}\frac{n_{\mathrm{c1}}(n_{\mathrm{c}}k_{\mathrm{c}}-(k_{\mathrm{c}}-2)n)+n_{\mathrm{c1}}^{2}-\Omega}{n_{\mathrm{c}}-n_{\mathrm{c1}}(k_{\mathrm{c}}-2)}\frac{N_{\mathrm{U}}}{2A_{\mathrm{a}}}, & 0\le n\le n_{\lambda},\\ f_{\mathrm{a}}, & n_{\lambda}\le n\le 1,\end{cases} \tag{5}$$

$$\sigma_{\mathrm{c}}=\begin{cases}\frac{n_{\mathrm{c}}(2n-n_{\mathrm{c1}}k_{\mathrm{c}})-n_{\mathrm{c1}}(k_{\mathrm{c}}-2)n+n_{\mathrm{c1}}^{2}+\Omega}{n_{\mathrm{c}}-n_{\mathrm{c1}}(k_{\mathrm{c}}-2)}\frac{N_{\mathrm{U}}}{2A_{\mathrm{c}}}, & 0\le n\le n_{\lambda},\\ \frac{N_{\mathrm{U}}n-A_{\mathrm{a}}f_{\mathrm{a}}}{A_{\mathrm{c}}}, & n_{\lambda}\le n\le 1,\end{cases} \tag{6}$$

where $\Omega=n_{\mathrm{c1}}\sqrt{(n_{\mathrm{c}}k_{\mathrm{c}}-(k_{\mathrm{c}}-2)n+n_{\mathrm{c1}})^{2}+4n(n_{\mathrm{c1}}(k_{\mathrm{c}}-2)-n_{\mathrm{c}})}$, $n_{\mathrm{c1}}=A_{\mathrm{a}}E_{\mathrm{a}}\varepsilon_{\mathrm{c1}}/N_{\mathrm{U}}$, $n_{\mathrm{c}}=A_{\mathrm{c}}f_{\mathrm{c}}/N_{\mathrm{U}}$, and n_{λ} is the normalized force for which steel yields,

$$n_{\lambda}=\frac{n_{\mathrm{c}}k_{\mathrm{c}}+n_{\mathrm{c1}}-n_{\mathrm{a}}(n_{\mathrm{c}}/n_{\mathrm{c1}}-k_{\mathrm{c}}+2)}{k_{\mathrm{c}}-2+n_{\mathrm{c1}}/n_{\mathrm{a}}}, \tag{7}$$

with $n_{\mathrm{a}}=A_{\mathrm{a}}f_{\mathrm{a}}/N_{\mathrm{U}}$. Solving $n_{\lambda}=1$ for f_{a} produces the formula for the maximum yield strength of steel, which should be taken in the cross-sectional analysis for a given concrete strength, so that the steel yields before peak stress in concrete is achieved and Eqs. (5) and (6) hold: $f_{\mathrm{a,max}}=E_{\mathrm{a}}\varepsilon_{\mathrm{c1}}$.

Now, let us consider a stress distribution function $\lambda(n)=\sigma_{\mathrm{a}}(n)/\sigma_{\mathrm{c}}(n)$ that illustrates the portion of the axial load carried by the steel and concrete parts of the composite cross-section for a given load level n. We can distinguish two characteristic values: the stiffness-based stress allocation $\lambda_{\mathrm{sb}}=\alpha$ resulting from the linear elastic analysis for force allocation, Eq. (2), and capacity-based stress allocation $\lambda_{\mathrm{cb}}=f_{\mathrm{a}}/f_{\mathrm{c}}$ for $n=1$. Note, that $\lambda(0)<\alpha$ as in the linear analysis a secant stiffness modulus E_{cm} is used, whereas on the onset of the loading path the initial tangent modulus of the concrete, $k_{\mathrm{c}}=1.05E_{\mathrm{cm}}$, drives the stress distribution function, cf. Fig. 1a. Also, both stiffness-based and capacity-based stress allocation values do not depend on ω, thus it makes it easier to contemplate the influence of the concrete nonlinearity, yielding of the steel, and aforementioned ω on the portion of the axial load carried by parts of the composite cross-section.

Until n reaches n_{λ}, the stress distribution curve is ascending because of the softening of concrete and for $n_{\lambda}<n\le 1$ the curve reverses since after the steel yields, only the concrete bears the additional axial load (Fig. 2). Finally, as n approaches unity, the stress distribution function λ tends to $\lambda_{\mathrm{cb}}=f_{\mathrm{a}}/f_{\mathrm{c}}$. The results suggest that for load levels $n<0.4$, the stiffness-based allocation of sectional forces is closer to the actual force distribution than the capacity-based force allocation. Therefore, for loads N_{Ed} lower than $0.4N_{\mathrm{U}}$, which corresponds to columns designed for global or local buckling ($\sigma_i<f_i$) or at service loads, the stiffness-based force allocation (2) should be utilized for establishing the design shear force. Note that N_{U} is significantly higher than $N_{\mathrm{pl,Rd}}$, thus the applicable ratio for which the stiffness-based solution (2) holds is even higher. The correspondence of the linear solution with the nonlinear model is better, the stronger the concrete and the weaker the steel used.

The effect of ω on $\lambda(n)$ is modest and amplified for larger values of n (Fig. 2). Therefore, the value of the ratio ω does not alter the previously formulated general condition that for $n<0.4$ a stiffness-based solution holds.

Even more disturbing are the stress distribution values for higher load levels, which are way beyond the bounds of the stiffness-based λ_{sb} and capacity-based λ_{cb} solutions. It is more concerning that, as

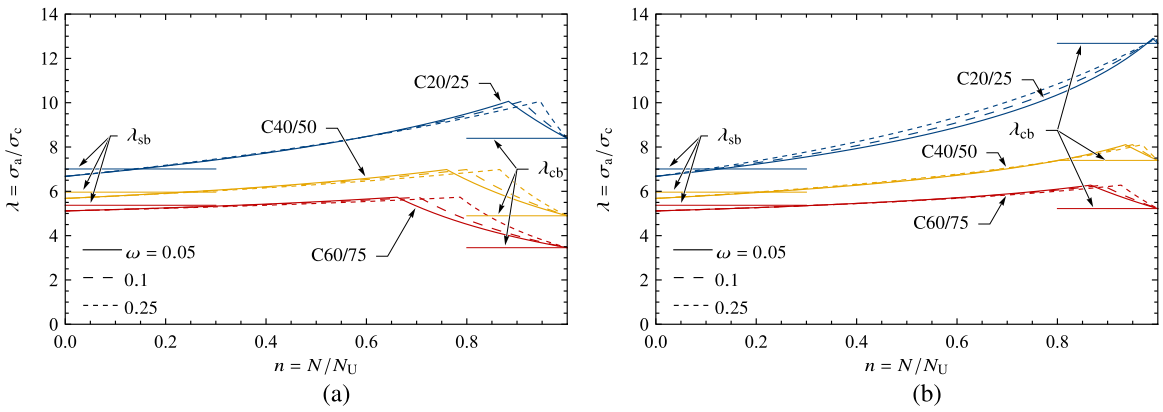

Fig. 2. Influence of $\omega = A_a/A_c$ on the stress distribution curve $\lambda(n)$ for (a) S235, (b) S355 steel.

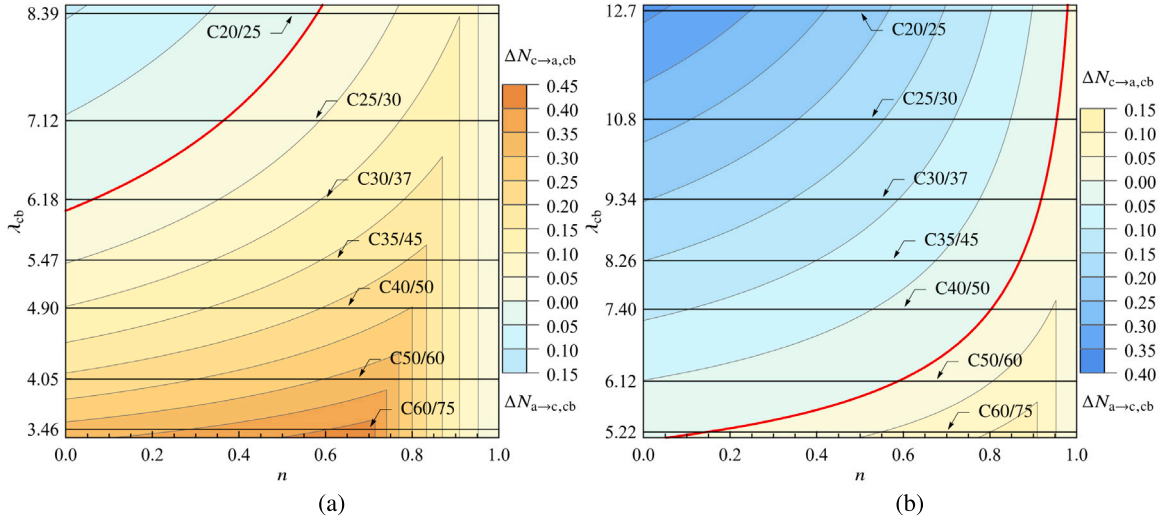

Fig. 3. Capacity-based force allocation underestimation error, calculated for (a) $f_a = 235$ MPa, (b) $f_a = 355$ MPa and $\omega = 0.1$.

stated above, N_U in nonlinear analysis of the cross-section is much higher than the assumed plastic resistance of the cross-section $N_{pl,Rd}$. Therefore, there is a risk that for the design resistance $N_{pl,Rd}$ of the cross-section in the ultimate limit state design scenario, the design shear force might be over or, even worse, underestimated depending on how the load is introduced to the composite cross-section. Especially the AISC Specification [2] requires designing the shear interface according to the capacity-based force allocation (1). The question arises, what error does this approach produce, and under what circumstances?

Let us consider, for the sake of argument, an initially stress-free column loaded through either concrete or steel. If the column is loaded through steel, a certain portion of the force has to be transferred to the concrete. Then, the shear force is equal to $V_{Ed} = N_c - 0 = A_c\sigma_c$. In that case, if $\lambda < \lambda_{cb}$, the capacity-based force allocation gives an unsafe estimation of the shear force. Similarly, if the force is transferred from concrete to steel, $V_{Ed} = A_a\sigma_a$, and for $\lambda > \lambda_{cb}$ the plastic solution gives an unsafe estimation of the shear force compared to the nonlinear method. The values of the force distribution from the nonlinear models, $N_{a,nl}$ and $N_{c,nl}$, can be calculated by multiplying the stresses σ_a and σ_c (Eqs. (5) and (6)) by A_a and A_c, respectively.

Fig. 3 shows the underestimation error of shear force when capacity-based force allocation is used for various load levels and λ_{cb}, corresponding to concrete grades as steel grade is fixed. Warm and cold colors characterize underrated shear force for loading through concrete and steel, respectively. The red contour line indicates the case when $\lambda = \lambda_{cb}$, thus the force distribution calculated with a nonlinear solution and capacity-based method is exactly the same. The underestimation error for composite columns loaded through steel, calculated with respect to capacity-based force allocation (1) is,

$$\Delta N_{a\to c,cb} = \frac{N_{c,nl} - N_{c,cb}}{N_{c,cb}} = \frac{\omega(\lambda_{cb} - \lambda)}{1 + \lambda\omega}, \tag{8}$$

and similarly, for loading through concrete,

$$\Delta N_{c\to a,cb} = \frac{N_{a,nl} - N_{a,cb}}{N_{a,cb}} = \frac{\lambda - \lambda_{cb}}{\lambda_{cb}(1 + \lambda\omega)}. \tag{9}$$

The major error, up to 35%, arises for weak steel and strong concrete when the load is introduced through concrete for $\omega = 0.1$ and n up to 0.4; conversely, when the load is introduced through steel to the composite cross-section, one should avoid a combination of higher steel grades and weak concrete, cf. Fig. 3a and b, respectively. As stated above, the change of ω does not alter the general conclusion that calculating the design shear force via the capacity-based force allocation may result in significant underestimation error, cf. Fig. 2. This is especially true for the load levels observed in slender columns and for service loads. However, we want to reiterate that also in the ultimate limit state we may be far from the actual force distribution because of the reduced value of the design concrete strength compared to the mean value of concrete strength.

Accordingly, let us investigate the underestimation error when the stiffness-based force allocation is adopted. Now, we compare the difference of the force in part of the composite cross-section obtained

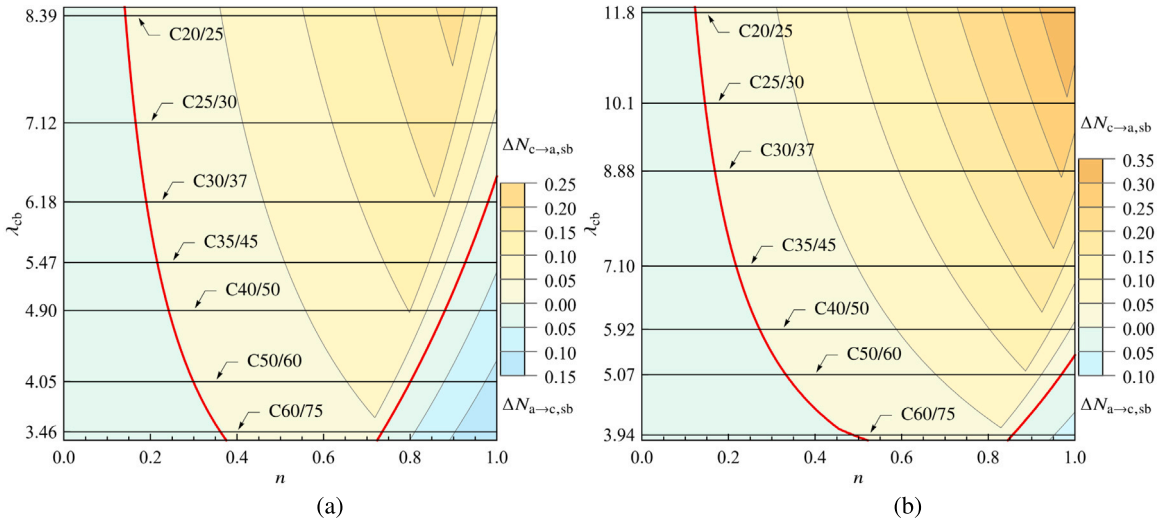

Fig. 4. Stiffness-based force allocation underestimation error, calculated for (a) $f_a = 235\,\text{MPa}$, (b) $f_a = 355\,\text{MPa}$ and $\omega = 0.1$.

with the nonlinear model of concrete and steel with the stiffness-based force allocation (2) with respect to the latter. Fig. 4 presents the underestimation errors both for loading through steel,

$$\Delta N_{a\to c,sb} = \frac{N_{c,nl} - N_{c,sb}}{N_{c,sb}} = \frac{\omega(\alpha - \lambda)}{1 + \lambda\omega}, \tag{10}$$

and concrete,

$$\Delta N_{c\to a,sb} = \frac{N_{a,nl} - N_{a,sb}}{N_{a,sb}} = \frac{\lambda - \alpha}{\alpha(1 + \lambda\omega)}, \tag{11}$$

for fixed steel grades, varying concrete grades, and for the same $\omega = 0.1$ as in Fig. 3. Again, the same convention applies as in capacity-based force allocation underestimation error: warm and cold colors denote loading through concrete and steel, respectively. The red contour line indicates the case when $\lambda = \lambda_{sb}$, thus the force distribution calculated with the nonlinear solution and stiffness-based force allocation is exactly the same. For loads n up to 0.4, the error between the stiffness-based force allocation and more precise nonlinear model is less than 5%, which is within the range of the engineering error. This proves that for the majority of design scenarios concerning slender columns and for service loads, rather the stiffness-based force allocation should be used instead of the capacity-based force allocation, which is recommended by AISC [2], to establish the design shear force.

The above deliberations tacitly disregard the long-term effects such as concrete creep. To include them in the analysis, one has to consider linear or nonlinear viscoelastic effects in concrete behavior, depending on the stress level in concrete [5]. Such analysis is out of scope of this paper, as we rather focus on the importance of stiffness of the shear connection in the load transfer area, for the sake of argument, in the transient design scenario and at low load levels. For persistent design situations, the concrete creep will affect the stiffness of the concrete component of the composite cross-section [26], thus impacting both stiffness-based force allocation (2) and the nonlinear solution, Eqs. (5) and (6).

3. Current rules for design of shear connectors

In Section 2 we have established the proper value of the design shear force for slender columns or at service loads. Following, we briefly review the current design rules [1,2] regarding the shear connection. In both design guides the strength of the shear connection is of central interest, while the stiffness demand is entirely neglected. This, in our opinion, is a major drawback considering that the shear connection should, apart from withstanding the load, be able to effectively distribute the introduced load between the composite cross-section components to attain the composite action of the column.

The first mechanism used to transfer the load is the natural bond between the steel and concrete. However, the AISC Specification [2] restrains the utilization of the natural bond to concrete-filled tubes, whereas the European standard [1] allows the natural bond mechanism both for concrete-filled and concrete-encased cross-sections. The maximal shear force transferred through the natural bond is limited by the transfer length L_t

$$V_{Rd} = \tau_{Rd} L_t \rho, \tag{12}$$

where ρ denotes the perimeter of the steel-concrete interface and the natural bond strength τ_{Rd} depends on the type of composite cross-section. The Eq. (12) is a result of a very simple rigid plastic model of the shear transferring mechanism, where the stiffness does not affect the result. Due to infinite stiffness the force is fully transferred provided that $V_{Ed} < V_{Rd}$. When the introduced load exceeds the shear connection strength V_{Rd}, or the natural bond is prohibited due to the cross-section type [2] or improper interface preparation [1], shear connectors are needed in a form of headed studs, welded channels, cold-formed angles, or other. Both standards [1,2] forbid superimposing the natural bond and shear connectors in the load transferring mechanism as the interaction of these two mechanisms is not fully understood and is a subject of ongoing research [27]. The experimental data [27] suggests that closely spaced shear connectors, as in the case of the load introduction area, are the main load bearer, which justifies the ban.

The design of the shear connectors stems from the same very simple rigid plastic model, where the design strength of the shear connection is a product of the strength of the connector P_{Rd} and the number of connectors m_p. This model is true as long as the shear connectors are ductile to enable the redistribution of the shear force [28]. The ductility requirement is fulfilled if the shear connector possesses the slip capacity of at least 6 mm [1], or the length to diameter ratio and other detailing requirements are met in the case of headed studs [2]. We will refer to this normative method of designing the shear connection as the Strength Method (StrM) for the obvious reason. Also, we will explore the shear connectors in a form of headed studs with the strength as specified by European standard [1],

$$P_{Rd} = \frac{1}{\gamma_v} \min\left(0.8 f_u \frac{\pi d^2}{4}; 0.29 \alpha d^2 \sqrt{f_{ck} E_{cm}}\right), \tag{13}$$

where $\gamma_V = 1.25$ is a partial safety factor and α depends on the ratio of the stud nominal height h_{sc} to diameter d,

$$\alpha = \begin{cases} 0.2\left(\frac{h_{sc}}{d}+1\right) & \text{for } 3 \le \frac{h_{sc}}{d} \le 4, \\ 1.0 & \text{for } \frac{h_{sc}}{d} > 4. \end{cases} \tag{14}$$

Eq. (13) holds for studs having diameter $16\,\text{mm} \le d \le 25\,\text{mm}$ and ultimate tensile strength $f_u \le 500\,\text{MPa}$. In other cases, the characteristic strength P_{Rk} of the shear connector should be established experimentally, see Annex B EN 1994-1-1 [1] or the relevant European Technical Assessment.

The AISC Specification [2] additionally provides the strength of steel channel connectors

$$P_{Rk} = 0.3\left(t_f + 0.5t_w\right) l_a \sqrt{f_c E_c}, \tag{15}$$

where t_f, t_w, denote channel's flange and web thickness, and l_a is the connector length.

The shear studs before yielding possess a certain stiffness, which is a well-established fact [29–31]. The influence of the shear studs' stiffness on the composite beams' behavior has been studied extensively [e.g., 32–34] with a focus on slip demand of studs and ultimate bending moment of the composite beams. However, applying the same design rules to the load transferring mechanisms in composite columns neglects the influence of the shear connection stiffness on the effectiveness of the introduced load distribution in the composite cross-section components, which we will investigate in the following section.

4. Analytical shear transfer models

To investigate the influence of the shear connection stiffness on the effectiveness of load transferring between the composite cross-section parts, we will employ a simple uniaxial bar model as our chief interest lays in load transferring and we do not consider bending effects. As proven in Section 2, for service loads or slender columns, the linear elastic relations for steel and concrete parts of the composite cross-section are adequate and will be assumed in this section.

The fundamental relation to solve the load transfer problem of the composite column is the balance of the forces in the infinitesimal slice of the column, cf. Fig. 5a,

$$\frac{\mathrm{d}N_i(x)}{\mathrm{d}x} \mp t(x) = 0, \tag{16}$$

where $t(x)$ is the unit shear force acting between the cross-section parts. For the part of the cross-section through which the load is introduced, the shear force decreases the axial force, thus the negative sign in Eq. (16). Conversely, the shear force increases the axial force in the part to which the load is transferred, leading to the plus sign in Eq. (16).

The solution to the Eqs. (16) depends on the assumed shear force slip law $t(s)$. In this paper we will consider three shear force slip laws: elastic, elastic plastic, and rigid plastic, cf. Fig. 5b. We consider only monotonic loading scenarios, thus we use a simplified version of deformation plasticity in the analytical solutions instead of the classic plasticity formulation with the typical loading/unloading conditions [35].

Let us discuss the applicability of the considered shear force slip laws. The rigid plastic like law, $t(s) = t_{Rd}$, represents the default model assumed in the current design guides [1,2] both for the natural bond and shear connectors as discussed extensively in Section 3. In this paper, we will consider this model only to represent the natural bond behavior both inside and outside of the load introduction area [19].

The elastic plastic like shear force slip law, $t(s) = \min\left(ks; t_{Rd}\right)$, where s denotes slip, describes the behavior of the shear connection with ductile shear studs. Both the stiffness k_{sc} and resistance P_{Rd} of the individual shear studs is transformed into smeared equivalents k, and t_{Rd}, respectively. Also, we neglect the increase of t_{Rd} stemming from the interaction of studs welded to the web with flanges of the I-section [1].

Lastly, we will adopt the linear elastic shear force slip law as a reference solution and, more significantly, a departure point for the construction of design charts ensuring assumed effectiveness of the design shear force transfer.

4.1. Closed form solutions

For definiteness, let us consider the shear transfer from the steel to the concrete part of the cross-section. Eqs. (16) with the linear elastic shear force slip model $t(x) = ks(x)$ and exploiting the linear constitutive relationships for both materials, $N_i = A_i\sigma_i$, where $\sigma_i = E_i u_i'$, become

$$\begin{aligned} \frac{\mathrm{d}^2 u_c(x)}{\mathrm{d}x^2} + \frac{k}{E_c A_c}\left(u_a(x) - u_c(x)\right) = 0, \\ \frac{\mathrm{d}^2 u_a(x)}{\mathrm{d}x^2} - \frac{k}{E_a A_a}\left(u_a(x) - u_c(x)\right) = 0. \end{aligned} \tag{17}$$

The same set of equations arises for transfer in the opposite direction: from the concrete to steel part of the cross-section as the sign of unit shear force $t(x)$ changes and simultaneously the slip definition changes to $s(x) = u_c(x) - u_a(x)$. Accordingly, the elastic branch of the elastic plastic model is governed by Eqs. (17). In general, the interface stiffness k might be a function of x, e.g., when shear studs are not spaced uniformly on the considered interval, but this case will not be pursued in this paper.

The homogeneous solution of Eqs. (17) is given as

$$\begin{aligned} u_{c0,el}(x) = E_a A_a \beta \Bigg[&\frac{1}{\alpha\omega}(B_1 + B_2 x) + (B_3 + B_4 x) \\ &+ (B_1 - B_3)\cosh(\beta x) + \frac{1}{\beta}(B_2 - B_4)\sinh(\beta x) \Bigg], \end{aligned} \tag{18}$$

$$\begin{aligned} u_{a0,el}(x) = E_c A_c \beta \Bigg[&(B_1 + B_2 x) + \alpha\omega(B_3 + B_4 x) \\ &+ (B_3 - B_1)\cosh(\beta x) + \frac{1}{\beta}(B_4 - B_2)\sinh(\beta x) \Bigg], \end{aligned} \tag{19}$$

where relative stiffness

$$\beta = \sqrt{k\left(\frac{1}{E_a A_a} + \frac{1}{E_c A_c}\right)} \tag{20}$$

and constants B_i are determined from the appropriate boundary and continuity conditions. Hegemier et al. [18] derived a similar set of differential equations to analyze the tension stiffening effect in reinforced concrete structures.

The solution of Eq. (16) for t reaching the limit value t_{Rd} in the rigid plastic model or in the plastic branch of the elastic plastic model is the same as for an uniaxial bar loaded with distributed load,

$$u_{c0,pl}(x) = -\frac{t_{Rd}}{2E_c A_c}x^2 + C_1 x + C_2, \tag{21}$$

$$u_{a0,pl}(x) = \frac{t_{Rd}}{2E_a A_a}x^2 + C_3 x + C_4. \tag{22}$$

Finally, the last part needed to compose the composite column problems' solutions is the case when $t = 0$, which corresponds to the rigid plastic solution below the yielded interface front. The homogeneous solution has the same form as in Eqs. (21) and (22) without the t_{Rd} term,

$$u_{c0,0}(x) = D_1 x + D_2, \tag{23}$$

$$u_{a0,0}(x) = D_3 x + D_4. \tag{24}$$

One readily recognizes the classic elastic solution of the uniaxial bar problem without distributed load. We will refer to this solution as a "bar solution" throughout this paper to distinguish from the elastic shear force slip law solution given by Eqs. (18) and (19).

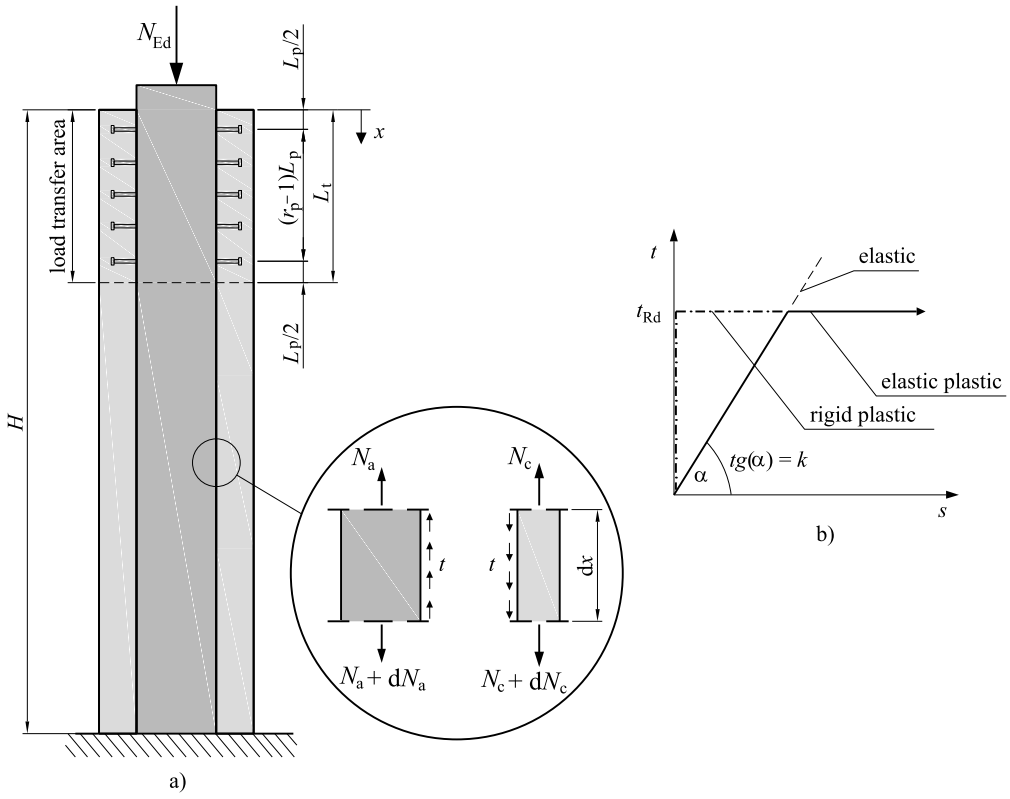

Fig. 5. Scheme of the force transfer problem (a) and considered shear force slip laws (b).

Table 1
Parameters of the composite column assumed in case studies.

Profile	Grade	E_i [GPa]	A_i [cm^2]	$f_{i,k}$ [MPa]	$f_{i,d}$ [MPa]	ω	α	ρ [cm]	τ_{Rd} [MPa]
HEA280	S355	210	97.3	355	355	5.84%	6.162	160.0	0.30
42 × 42 cm	C35/45	34.08	1666.7	35	23.33				

The last missing part needed for the analysis of the load transfer problem is the stiffness of the shear studs. According to EN 1994-1-1 [1], the stiffness of the shear connector may be taken as $0.7P_{Rk}/s$, where s is the slip determined from push-out tests in accordance with Annex B [1] at load $0.7P_{Rk}$. EN 1994-1-1 [1] provides an approximate value of shear connector stiffness, $k_{sc} = 100\,\text{kN/mm}$ for headed studs of 19 mm in diameter and $k_{sc} = 70\,\text{kN/mm}$ for cold formed angles. In the literature, different formulae for the stiffness of shear studs based on the experimental and FEM results can be found [e.g. 29,36–38]. In this paper, for the sake of the argument, we assume the headed studs have $d_{sc} = 19\,\text{mm}$, $h_{sc} = 60\,\text{mm}$, and stiffness $k_{sc} = 100\,\text{kN/mm}$.

4.2. Case studies

Let us consider a concrete encased HEA280 profile of height $H = 3\,\text{m}$ loaded through steel in a different design scenarios with material parameters (Table 1) according to European standards [1,5,6]. Adopted geometrical properties, materials parameters, and a maximum axial load of $N_{Ed,max} = 3400\,\text{kN} \approx 0.32N_U \approx 0.5N_{pl,Rd}$ considered ensure that the steel part does not yield when loaded ($N_{Ed,max}/A_a = 349.4\,\text{MPa} < f_a$) and the stress in concrete calculated via stiffness-based force allocation (2) is at a relatively low level ($\sim 15\,\text{MPa}$). For the sake of clarity, the reinforcement is disregarded.

The European standard [1] limits the transfer length L_t to a minimum of $H/3 = 1\,\text{m}$ and $2D = 84\,\text{cm}$, thus, $L_t = 2D = 0.28H = 84\,\text{cm}$ is assumed. The design resistance of the load introduction area exploiting the natural bond (12) is equal to

$$V_{Rd} = t_{Rd}L_t = 403.2\,\text{kN}, \tag{25}$$

where $t_{Rd} = \tau_{Rd}\rho = 4.80\,\text{kN/cm}$. Let us consider an axial load for which the design shear force per stiffness-based force allocation (2) equals V_{Rd}, thus

$$N_{c,sb} = V_{Rd} \quad \rightarrow \quad N_{V,Rd} = (1 + \alpha\omega)V_{Rd} = 548.3\,\text{kN}. \tag{26}$$

We assume a rigid plastic shear force slip model for the natural bond mechanism. Therefore, the solution is a combination of the plastic solution (Eqs. (21) and (22)) in the load introduction area and the bar solution (Eqs. (23) and (24)) otherwise. Applying the following boundary and continuity conditions

$$\begin{aligned} E_aA_au'_{a0,pl}(0) &= -N_{Ed}, & E_cA_cu'_{c0,pl}(0) &= 0,\\ u_{a0,0}(H) &= 0, & u_{c0,0}(H) &= 0,\\ u_{a0,pl}(x_A) &= u_{a0,0}(x_A), & u_{c0,pl}(x_A) &= u_{c0,0}(x_A),\\ E_aA_au'_{a0,pl}(x_A) &= E_aA_au'_{a0,0}(x_A), & E_cA_cu'_{c0,pl}(x_A) &= E_cA_cu'_{c0,0}(x_A), \end{aligned} \tag{27}$$

solves the problem at hand, where $x_A = \min\left(N_{Ed}/\left(t_{Rd}(1+\alpha\omega)\right); L_t\right)$, denotes the extent of the yielded interface.

The assumed rigid plastic model in the introduction length guarantees that the axial load is properly distributed (Fig. 6) for any load smaller than $N_{V,Rd}$ given by Eq. (26). When the axial load exceeds the design resistance of the load introduction area, e.g., $N_{Ed} = 2N_{V,Rd}$, only the portion of the load equal to the resistance is transferred to the concrete part. This results in partial force transfer (Fig. 6a, $\eta = 2$). The extent of the load transfer area is rather arbitrary, therefore the shear force would surpass the load transfer area and the full composite action would be achieved if the column is tall enough. However, this would deprive the interface of its capacity to withstand additional shearing

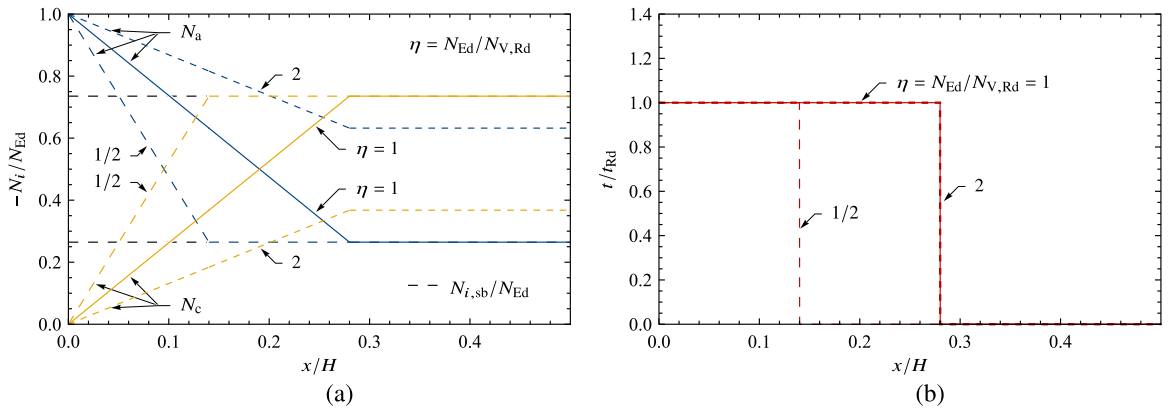

Fig. 6. Rigid plastic model solutions describing natural bond mechanism in the load introduction area: cross-sectional forces (a) and unit shear force $t(x)$ distribution (b).

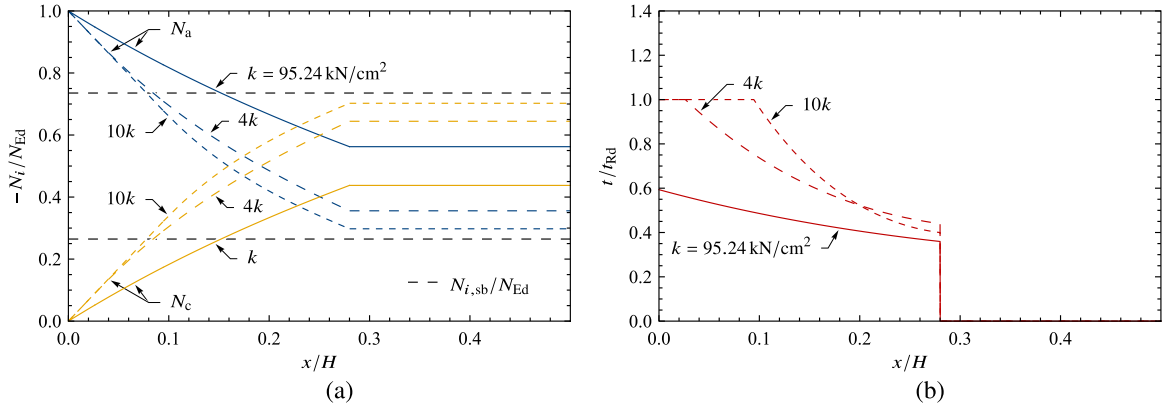

Fig. 7. Elastic plastic model solutions describing shear studs behavior in the load introduction area: cross-sectional forces (a) and shear force $t(x)$ distribution (b) with different stiffness k and constant design shear resistance t_{Rd}.

resulting from the bending of the column or incipient buckling, and is generally not desired [1].

Now, let us assume that for the same load $N_{V,Rd}$ the designer decides to use shear studs grade S235 to transfer shear force V_{Ed}. The design resistance of the shear stud, (13), yields $P_{Rd} = 65.3\,kN$. Following the Strength Method (StrM), the required number of studs m_p is,

$$m_p = n_p r_p > \frac{V_{Ed}}{P_{Rd}} = 6.17. \tag{28}$$

Arranging the studs pairwise ($n_p = 2$) results in $r_p = 4$ layers, thus the layers' spacing is $L_p = L_t/r_p = 21\,cm$. The averaged value of stiffness and design resistance of the interface are equal to, cf. Fig. 5,

$$\begin{aligned} k &= \frac{n_p k_{sc}}{L_p} = \frac{m_p k_{sc}}{L_t} = 95.24\,kN/cm^2, \\ t_{Rd} &= \frac{n_p P_{Rd}}{L_p} = \frac{m_p P_{Rd}}{L_t} = 6.22\,kN/cm. \end{aligned} \tag{29}$$

The smeared design resistance of the interface t_{Rd} is $\approx 9\%$ higher than in the case of the natural bond mechanism but now the shear connection has a certain stiffness. This means that only after mobilization of enough slip, the interface will reach the design resistance. In the load transfer problem, the slip is a function of the axial stiffness of the composite cross-section parts and interface stiffness. This distinguishes the composite columns from the composite beams, where the slip is a result of bending and its mobilization is fairly easy.

It is not known from the onset, if for a given load the design resistance would be achieved. However, for a given column, shear connection stiffness, and design resistance t_{Rd}, one can calculate the axial load $N_{Ed,el}$ initiating yielding of the interface ($t(0) = t_{Rd}$) combining elastic shear force slip (Eqs. (18) and (19)) and bar solutions (Eqs. (23) and (24)):

$$\begin{aligned} &E_a A_a u'_{a0,el}(0) = -N_{Ed}, && E_c A_c u'_{c0,el}(0) = 0, \\ &u_{a0,0}(H) = 0, && u_{c0,0}(H) = 0, \\ &u_{a0,el}(L_t) = u_{a0,0}(L_t), && u_{c0,el}(L_t) = u_{c0,0}(L_t), \\ &E_a A_a u'_{a0,el}(L_t) = E_a A_a u'_{a0,0}(L_t), && E_c A_c u'_{c0,el}(L_t) = E_c A_c u'_{c0,0}(L_t), \end{aligned} \tag{30}$$

and

$$t(0) = k s(0) = k\left(u_{a0,el}(0) - u_{c0,el}(0)\right) = t_{Rd}. \tag{31}$$

Solving Eqs. (30) and (31) gives

$$\begin{aligned} N_{Ed,el,a} = -N_a(0) &= \frac{(H - L_t)\beta + \coth(\beta L_t)}{1 + (H - L_t)\beta \coth(\beta L_t)} \frac{t_{Rd}}{k} \beta E_a A_a \\ &= 924.23\,kN > N_{V,Rd}. \end{aligned} \tag{32}$$

Thus, the considered axial load $N_{V,Rd}$ is insufficient to mobilize the design resistance of the interface with shear studs, cf. Fig. 7b.

Moreover, the number of studs resulting from the StrM allow only to transfer shear force $V = -N_c(L_t) = 239.94\,kN$. The portion of the shear force that the shear connection failed to transfer reaches $(V_{Ed} - V)/V_{Ed} \approx 40\%$. Comparing this result with the effectiveness of the natural bond mechanism is concerning.

The reason for the apparent paradox that enhancing the shear connection with shear studs deteriorates the load transferring mechanism is twofold. Apparently, as the spacing of the studs is significant, the interaction between the natural bond and studs occurs [27], but this utilization is forbidden in the design guides [1,2]. Also, we assume that the natural bond interface is perfectly rigid up to reaching its design resistance. The limited data is available in the literature regarding the pure shear behavior of the steel-concrete interface. The

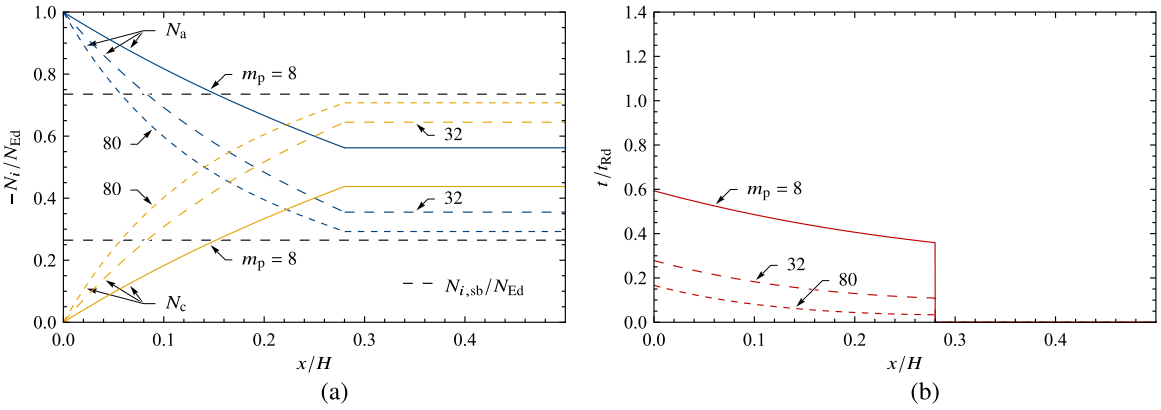

Fig. 8. The effect of increasing the number of studs in the load introduction area for load $N_{V,Rd}$: cross-sectional forces (a) and unit shear force $t(x)$ distribution normalized by the corresponding $t_{Rd} = m_p P_{Rd}/L_t$ (b).

only contribution we are aware of is that of Wium [17] reported in Wium and Lebet [3], where the author established the natural bond modulus $S = 500\,\mathrm{N/mm^3}$. The equivalent interface stiffness of the natural bond equals $k_{nb} = S\rho = 80\,\mathrm{MN/cm^2}$, which is a thousandfold times higher than smeared shear studs interface stiffness k but still a finite value which would affect the axial load transferring. Nevertheless, because of the considerable difference between the stiffnesses, we believe that the rigid plastic model for the natural bond may be an adequate assumption, cf. [19], at least until more experimental evidence accumulates. Also, the experimental results for axially loaded columns [39] indicates that that debonding progresses along the column with increasing load. The discussion regarding the fluctuations of the τ_{Rd} during slippage, resulting from the change in mechanism at microscale (micro/macro-locking) and frictional effects, is out of scope of this paper. We assume a constant, lower bound value of τ_{Rd} given by the European standard [1].

Increasing the stiffness of the shear connection changes the shear force distribution in the load introduction area (Fig. 7b). Quadrupling the stiffness and keeping the design shear resistance initiates yielding of the shear interface. Now, the solution is a combination of the plastic shear force slip model (Eqs. (21) and (22)) up to the end of the yielded interface ($x_A < L_t$), the elastic shear force slip model for the remainder of the load introduction area (Eqs. (18) and (19)), and the bar solution outside the load introduction area (Eqs. (23) and (24)). The boundary and continuity conditions yield the following set of equations,

$$\begin{aligned}
E_a A_a u'_{a0,pl}(0) &= -N_{Ed}, & E_c A_c u'_{c0,pl}(0) &= 0,\\
u_{a0,0}(H) &= 0, & u_{c0,0}(H) &= 0,\\
u_{a0,pl}(x_A) &= u_{a0,el}(x_A), & u_{c0,pl}(x_A) &= u_{c0,el}(x_A),\\
E_a A_a u'_{a0,pl}(x_A) &= E_a A_a u'_{a0,el}(x_A), & E_c A_c u'_{c0,pl}(x_A) &= E_c A_c u'_{c0,el}(x_A),\\
u_{a0,el}(L_t) &= u_{a0,0}(L_t), & u_{c0,el}(L_t) &= u_{c0,0}(L_t),\\
E_a A_a u'_{a0,el}(L_t) &= E_a A_a u'_{a0,0}(L_t), & E_c A_c u'_{c0,el}(L_t) &= E_c A_c u'_{c0,0}(L_t),
\end{aligned} \tag{33}$$

where x_A has to be calculated numerically from

$$k\left(u_{a0,el}(x_A) - u_{c0,el}(x_A)\right) = t_{Rd}, \tag{34}$$

which produces

$$k\frac{\beta(H-L_t)\coth\left(\beta(L_t-x_A)\right)+1}{\coth\left(\beta(L_t-x_A)\right)+\beta(H-L_t)} = \frac{E_a A_a t_{Rd}\beta}{N_{Ed} - t_{Rd}x_A(1+\alpha\omega)}. \tag{35}$$

A further increase in stiffness, e.g., tenfold allows more effective utilization of the shear connection capacity. In general, the greater the stiffness of the connection the better the axial load distribution among the composite cross-section parts, cf. Fig. 7a.

However, the change of the stiffness usually entails the change of the design resistance of the shear connection. For a given shear stud's type, increasing the number of studs m_p leads to a proportional increase of the interface stiffness k and design resistance t_{Rd}, cf. Eq. (29). On the other hand, the shear force $V = -N_c(L_t)$ cannot surpass the value when the full shear transfer is attained $N_{Ed}/(1+\alpha\omega)$ for loading through steel. Therefore, $\mathrm{d}V/\mathrm{d}m_P \to 0$ as $m_p \to \infty$, while the load introduction area capacity $\mathrm{d}(t_{Rd}L_t)/\mathrm{d}m_P = P_{Rd} = \text{const}$, which leads to conclusion that with increasing number of studs the shear force transfer improves (Fig. 8a), yet the utilization of the shear interface capacity decreases (Fig. 8b). This observation encourages utilizing the elastic shear force slip law to establish a guideline for required shear connection stiffness to effectively transfer the shear force between the composite cross-section parts, cf. Section 5.2.

Now, let us investigate the shear connection behavior at much higher axial load, $N_{Ed} = N_{Ed,max} = 3400\,\mathrm{kN}$. The design shear force from the stiffness-based force allocation (2) equals $V_{Ed} = 2500.3\,\mathrm{kN}$. Therefore, the required number of studs m_p per StrM has to be greater than $V_{Ed}/P_{Rd} \approx 38.3$. Assuming $m_p = 40$ studs, the smeared stiffness k and design resistance t_{Rd} are equal to $476.19\,\mathrm{kN/cm^2}$ and $31.10\,\mathrm{kN/cm}$, respectively.

For higher axial load, the load transfer is more effective because of the higher stiffness of the shear connection resulting from the capacity demand of the StrM, cf. Fig. 9a. Also, the partial utilization of the shear connection occurs (Fig. 9b). However, there is still a portion of the design shear force V_{Ed} that was not conveyed in the load introduction area, $(V_{Ed} - V)/V_{Ed} \approx 10.9\%$.

The design guides [1,2] forbid to transfer shear force outside the load introduction area. Nevertheless for finite stiffness of the shear connection, the full transfer is hardly attainable. In the real-world, however, one expects that either the natural bond or loosely spaced shear studs will take part in the force transferring mechanism. The goal is to limit the unconveyed part of the shear force, so that the column acts as a composite member and other mechanisms (natural bond or shear connectors) allow the column to withstand shearing from other sources.

Accordingly, let us consider how far, for the given axial load $N_{Ed,max}$, the natural bond mechanism has to be mobilized to transfer the remaining part of the shear force. It appears that exploiting of the natural bond diminishes the utilization of the shear connection in the load introduction area (Fig. 10b). Moreover, around 40% of the column height outside of the load introduction area is used to transfer the remaining shear force, cf. Fig. 10, thus, effectively, the column loses the ability to transfer any additional shear loads either from the column bending or incipient buckling.

Further, we analyzed how the assumed simplification of the linear elastic constitutive relations for steel and concrete affects the load transferring mechanism. The nonlinear stress–strain concrete law, Eq. (3), and elastic plastic model for steel (Fig. 1b) together with considered shear force slip laws (Fig. 5b) require resorting to numerical

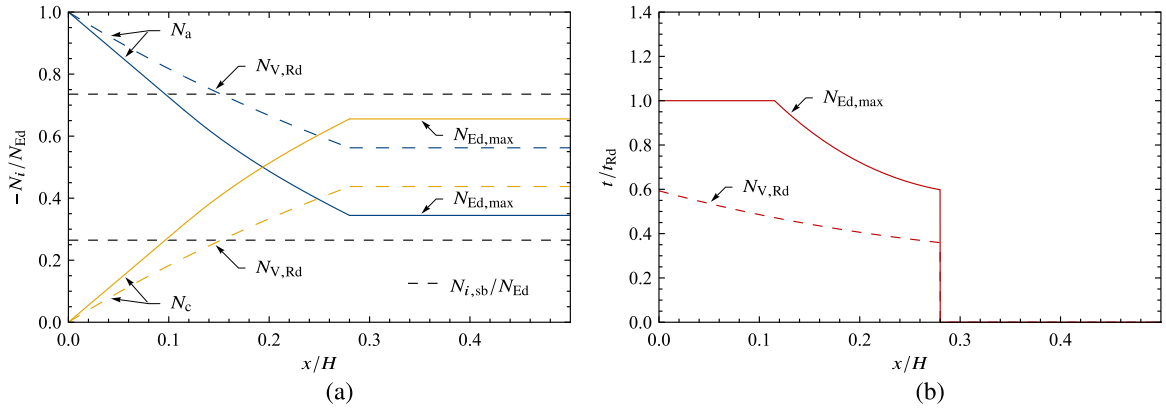

Fig. 9. The resulting cross-sectional forces (a) and unit shear force $t(x)$ (b) from StrM shear studs design for different load levels: $N_{V,Rd}$ ($m_p = 8$) and $N_{Ed,max}$ ($m_p = 40$).

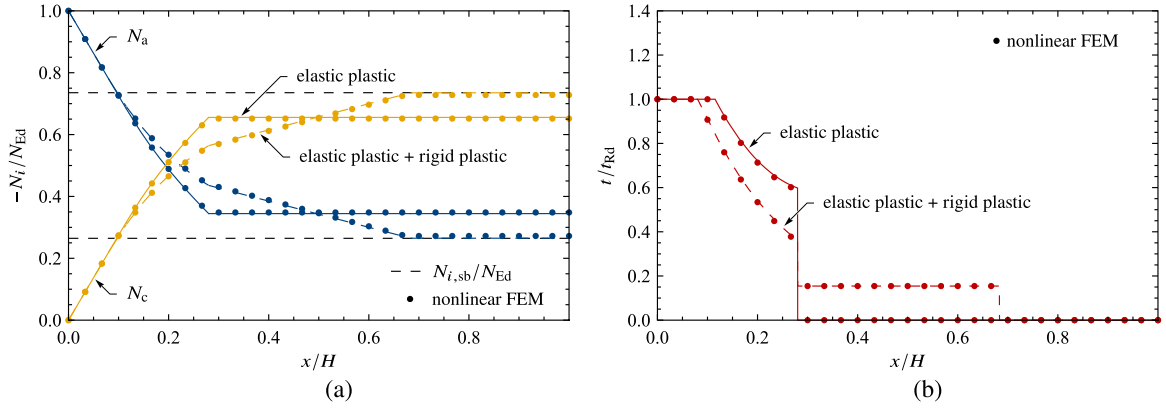

Fig. 10. The exploiting of the natural bond influence on the cross-sectional forces (a) and shear force $t(x)$ (b) and comparison with the nonlinear FEM results for $N_{Ed,max}$. The every tenth point of the FEM results is shown for clarity.

methods, e.g., the Finite Element Method (FEM). The necessary finite elements of 1D rods with quadratic shape functions were implemented in the *AceGen/AceFEM* system [40] following the standard approach. To represent the concrete and steel parts of the cross-section we used 300 finite elements for each part. The interaction between the cross-section components was enforced nodewise via the following methods. For elastic shear force slip law, the penalty-like potential was used $\Pi_{pen} = k(u_a - u_c)^2/2$, where the penalty parameter is interpreted as the interface stiffness k. Adding plasticity to the elastic shear force slip law results in the typical trial and radial return scheme for unit shear t. Lastly, for rigid plastic shear force slip law, the slip-stick conditions were enforced with the augmented Lagrangian method [41], similar as in the contact problems [42,43].

The difference between the analytical solutions obtained with linear elastic constitutive relations and the nonlinear FEM results is almost indistinguishable for the considered column loaded through steel (Fig. 10). The relatively low stress in the concrete after the full shear force transfer (≈15 MPa) does not affect the solution. The most pronounced difference emerges in the ratio $-N_i/N_{Ed}$ after the full shear force transfer in the case of natural bond usage, which is slightly different from $N_{i,sb}/N_{Ed}$. This is a result of the nonlinearity of the concrete model, which was discussed extensively in Section 2.

The more pronounced difference is expected in the case when the column is loaded through concrete. The axial load $N_{Ed,max}$ produces $\sigma_c = N_{Ed,max}/A_c \approx 20.4\,\text{MPa} \approx 0.87 f_{cd}$. Now, the designer following the StrM would calculate only 14 studs to transfer the design shear force $V_{Ed} = N_{Ed,max}\alpha\omega/(1+\alpha\omega) = 899.7\,\text{kN}$. This results in the smeared stiffness $k = 166.7\,\text{kN/cm}^2$ and design resistance $t_{Rd} = 10.88\,\text{kN/cm}$, which are significantly lower values than in the case of loading through steel.

The discrepancy between the results obtained with the linear elastic and non linear constitutive relations for the composite cross-section parts increased, yet still is not significant from the engineering point of view (Fig. 11). The difference is especially visible in the shear force distribution, cf. Fig. 11b. The closer the stress in the concrete from the axial load N_{Ed} is to the mean compressive strength of the concrete f_{cm}, used in Eq. (3), the more noticeable the difference between the two solutions. However, as the concrete usually is the main bearer of the load in the composite cross-section, we will approach the regime closer to the ultimate axial load N_U, which is rarely attainable in slender columns or at service loads.

In the considered loading through the concrete, without including the natural bond outside the load introduction area, we obtain the unconveyed shear force portion of $(V_{Ed} - V)/V_{Ed} = 27\%$. We want to reiterate that designing the studs per StrM leads to insufficient load transfer in the load introduction area. In the following section, we propose a novel Stiffness Method (StiffM) to circumvent this issue.

5. Stiffness method

5.1. Shear demand condition

It is important to note that using the elastic plastic model for the shear force slip mechanism, either utilizing only the elastic branch or both elastic and plastic branches, the full composite action is never reached. The full shear force transfer is an asymptote of the elastic plastic model solution. As mentioned before, the remaining part of the shear force will be transferred through natural bond or loosely spaced shear studs outside the load introduction area. In derivation of the shear demand condition, we focus only on the shear force transferred in the

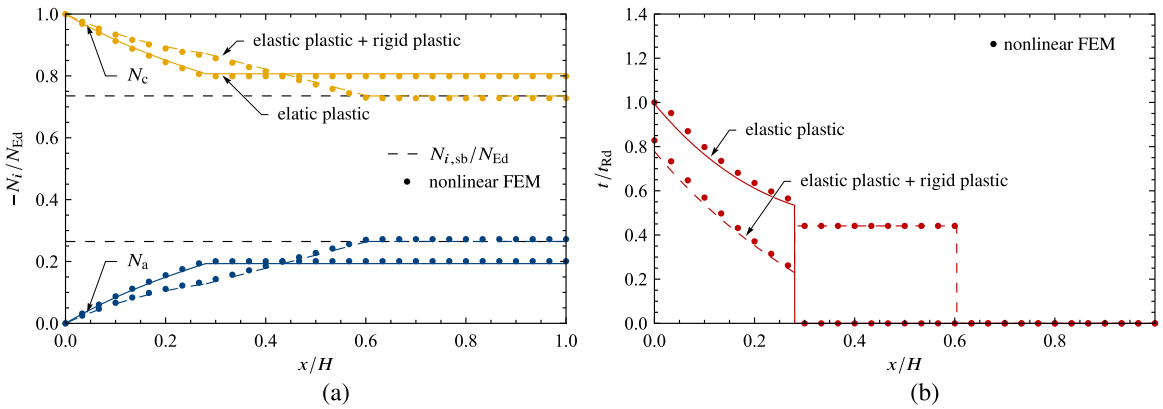

Fig. 11. The influence of the concrete nonlinearity when the column is loaded through concrete on the cross-sectional forces (a) and shear force $t(x)$ (b) for $N_{Ed} = 4400\,\mathrm{kN}$. The every tenth point of the FEM results is shown for clarity.

load introduction area. Thus, in the following considerations k and t_{Rd} outside the load introduction area are equal to zero.

To limit the unconveyed force by the shear connection, we propose to introduce the shear demand ratio,

$$\kappa = \frac{V}{V_{Ed}}, \tag{36}$$

describing the ratio of the shear force transferred in the load introduction area V to the design shear force V_{Ed} resulting from the stiffness-based force allocation, cf. Eq. (2). In the case of the initially unloaded column, V_{Ed} equals $N_{c,sb}$ and $N_{a,sb}$ for the load introduction through steel and concrete, respectively. Likewise, the actually conveyed shear force V equals to the axial force in the corresponding part of the cross-section, $N_i(x)$, where $x \geq L_t$ as the axial force is constant outside the load introduction area.

Let us calculate the aforementioned axial force outside the load introduction area with the elastic shear force slip law. Thus, exploiting the fact that the elastic shear force slip model solution (Eqs. (18) and (19)) does not depend on to which part of the cross-section the load in introduced, one can solve the Eqs. (30), which correspond to loading through steel. Then, the transferred shear force,

$$V = -N_c(L_t) = \frac{N_{Ed}}{1+\alpha\omega}\left(1 - \frac{1}{\cosh(\beta L_t) + (H - L_t)\sinh(\beta L_t)}\right), \tag{37}$$

where one readily recognizes factor $N_{Ed}/(1+\alpha\omega)$ as the stiffness-based force allocation $N_{c,sb} = V_{Ed}$. Consequently, the shear demand condition (36) becomes

$$\kappa = \frac{-N_c(L_t)}{N_{c,sb}} = 1 - \frac{1}{\cosh(\beta L_t) + (H - L_t)\sinh(\beta L_t)}. \tag{38}$$

Remarkably, Eq. (38) does not depend on the considered axial load level and, as stated above, the direction of the load introduction.

For a given column height H, transfer length L_t and desired shear demand κ, one can calculate from Eq. (38) the relative stiffness $\beta = \beta_{min}$ using numerical methods, as Eq. (38) is of the transcendental type. Then, from the required relative stiffness β_{min}, using material parameters (E_i, A_i) and Eq. (20), one can establish the required minimal shear connection stiffness

$$k_{min} = \beta_{min}^2 \frac{E_a A_a E_c A_c}{E_a A_a + E_c A_c}, \tag{39}$$

which for given shear connectors stiffness k_{sc} results in the required number of studs

$$m_p \geq \frac{k_{min}}{k_{sc}} L_t. \tag{40}$$

Then, following Eq. $(29)_1$ the actual smeared shear connection stiffness is established and $k > k_{min}$. This novel approach, we denote as the Stiffness Method (StiffM).

We provide design charts for the shear demand $\kappa = 0.90$, 0.925, 0.95, and 0.975 presenting the required relative stiffness β for a given column height H and ratio L_t/H (Fig. 12). The remainder of the shear force may be transferred via natural bond between steel and concrete assuming $t_{Rd} = \tau_{Rd}\rho$ or other means, e.g., properly designed shear connectors outside the load introduction area. Using the shear demand, the designer can make an informed choice whether the extent of natural bond mobilization, which can be estimated as

$$L_{nb} \approx \frac{(1-\kappa)V_{Ed}}{\tau_{Rd}\rho}, \tag{41}$$

is acceptable. It is a rough estimate as the natural bond utilization outside the load introduction area slightly decreases the shear force transferred in it, cf. Figs. 10b and 11b, thus, the actual extent is greater. Nevertheless, if the designer decides that the extent of L_{nb} is not acceptable, one can resort to higher shear demand.

The required relative stiffness β for a given ratio L_t/H is lower for taller columns. This demonstrates the influence of the axial stiffness of the composite cross-section parts. For taller columns, the top displacement is greater than for the shorter ones, thus, the more slip. Since the shear force depends on the slip, consequently there is better shear force transfer. As a result, more force will be transferred for a taller, more axially compliant column, with the same absolute transfer length and interface stiffness. On the other hand, reducing the stiffness of the interface in proportion to the increased length of the column, e.g., doubling the column height and halving the interface stiffness, results in significantly different slips in both columns, but similar force transfer for the considered parameters.

It might raise concerns if establishing the relative stiffness β, and in effect the smeared shear connection stiffness k, from the elastic shear force slip law model is feasible. One can readily check if for established k and t_{Rd} (through Eqs. (29)) from the required β, the elastic shear force slip law in the load introduction area holds by comparing the introduced axial load N_{Ed} with the axial load initiating yielding of the interface $N_{Ed,el}$, via Eq. (32) for loading through steel, and

$$N_{Ed,el,c} = \frac{(H - L_t)\beta + \coth(\beta L_t)}{1 + (H - L_t)\beta\coth(\beta L_t)} \frac{t_{Rd}}{k} \beta E_c A_c \tag{42}$$

for loading through concrete.

If $N_{Ed} \leq N_{Ed,el}$, the interface works in the elastic domain and the design is complete. On the other hand, when $N_{Ed} > N_{Ed,el}$ the designer has two alternatives. First (StiffM fast), to increase the number of studs, thus k and t_{Rd}, until $N_{Ed} \leq N_{Ed,el}$. Second (StiffM detailed), find the elastic plastic solution, Eqs. (33) and (35), for loading through steel and corresponding set of equations for loading through concrete. The comparison of these two alternatives is presented in Section 5.2 for the considered design example.

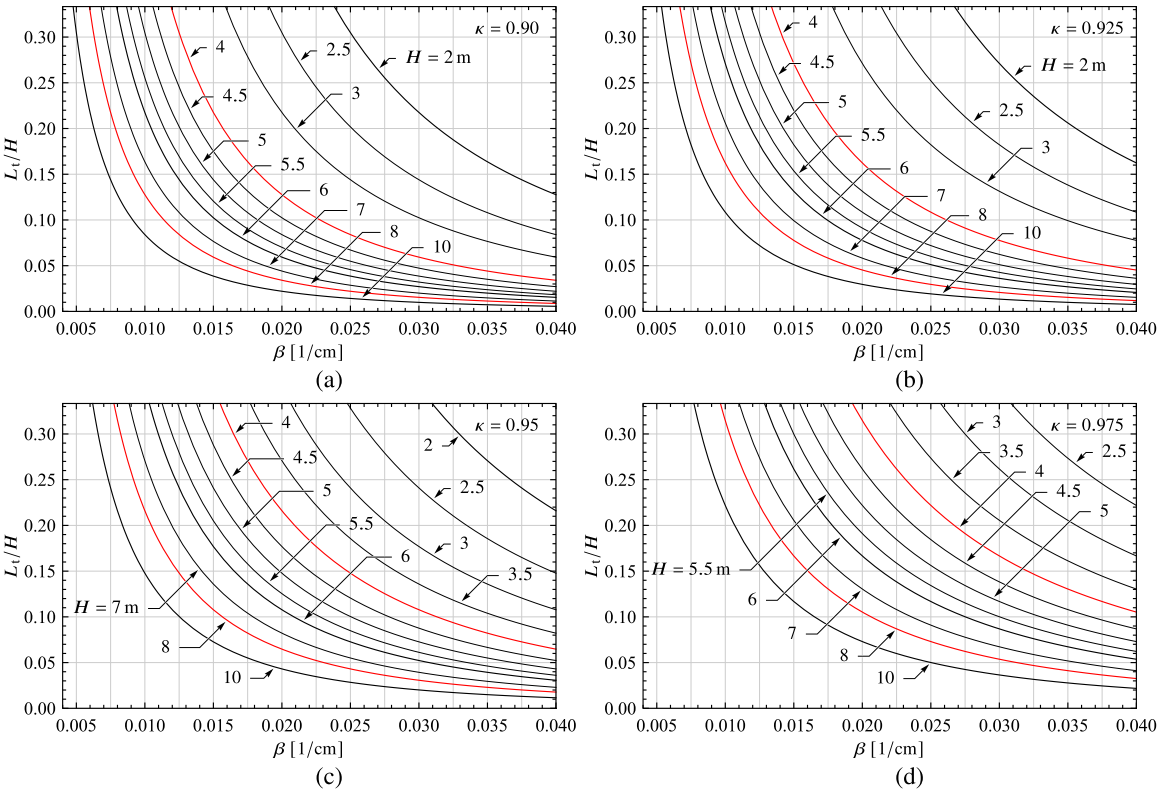

Fig. 12. The design charts for the column head stiffness according to StiffM calculated for $\kappa = 0.90$ (a), 0.925 (b), 0.95 (c), and 0.975 (d).

For the sake of completeness, we provide the shear demand ratio for partially yielded interface, κ_{ep}, for the load introduction through steel,

$$\kappa_{ep,a\to c} = \frac{N_c(L_t)}{N_{c,sb}} = 1 - \frac{1 - t_{Rd}x_A(1+\alpha\omega)/N_{Ed}}{\cosh\left((L_t - x_A)\beta\right) + (H - L_t)\beta\sinh\left((L_t - x_A)\beta\right)}, \tag{43}$$

and concrete

$$\kappa_{ep,c\to a} = \frac{N_a(L_t)}{N_{a,sb}} = 1 - \frac{1 - t_{Rd}x_A(1+\alpha\omega)/\left(N_{Ed}\alpha\omega\right)}{\cosh\left((L_t - x_A)\beta\right) + (H - L_t)\beta\sinh\left((L_t - x_A)\beta\right)}, \tag{44}$$

where x_A denotes the extent of the yielded interface, cf. Fig. 5. For loading through steel, x_A has to be calculated from Eq. (35) after solving Eqs. (33), and their counterparts for loading through concrete. In that case, in the right hand side of Eq. (35) E_aA_A changes to E_cA_c and $(1 + \alpha\omega)$ has to be replaced with $(1 + \alpha\omega)/(\alpha\omega)$. The solution is challenging, but finishing the design without checking κ_{ep} may lead to unsatisfactory shear transfer as κ_{ep} is always lower than κ for given β and $N_{Ed} > N_{Ed,el}$.

5.2. Application to load introduction design

Let us compare the results obtained with the proposed stiffness and standard strength method for the column from Section 4.2 for $N_{Ed} = N_{Ed,max} = 3400\,\text{kN}$. The StrM method required a minimum 38.3 studs, and we adopted $m_p = 40$ with entailing shear interface stiffness k and resistance t_{Rd} through Eqs. (29). As the calculated number of studs involve a partial yielding of the interface (Fig. 9b), one can calculate the shear demand and estimate of the length of the natural bond mobilization through Eqs. (41) and (43), respectively.

Now, let us assume we want to attain the shear demand $\kappa = 0.95$. Using the design chart (Fig. 12c) for $H = 3\,\text{m}$ and $L_t/H = 0.28$, we estimate the minimum relative stiffness $\beta_{min} = 0.023\,1/\text{cm}$. For the given studs, hence stiffness k_{sc} and capacity P_{Rd}, one can readily transform β_{min} into the required minimum number of studs (Eqs. (39) and (40)), which yields 66.8. Assuming $m_p = 68$, with the aid of Eqs. (29) and (32) we calculate $N_{Ed,el} = 3014.2\,\text{kN} < N_{Ed}$. Thus, the required relative stiffness β_{min} read from the design chart is too low for the considered N_{Ed} to attain exactly the desired shear demand. Moreover, to calculate the obtained shear demand κ_{ep}, one has to solve the set of Eqs. (33) and (35).

The indicator if the shear demand κ_{ep} might differ substantially from the desired value is the considerable difference between $N_{Ed,el}$ and N_{Ed}. In the considered case $N_{Ed,el}$ is close to N_{Ed}, hence the expected extent of yielded interface is not significant and κ_{ep} should not differ considerably from the desired value 0.95. In fact, in the design process one usually adopts a number of studs greater than what is required by β_{min} (here $m_p = 68 > 66.8$) which produces $\kappa_{ep} = 0.952$ and satisfies the initial requirement $\kappa = 0.95$. However, note that this is a particularity for the considered example.

The alternative to solving Eqs. (33) and (34) is to increase the number of studs to achieve $N_{Ed,el} > N_{Ed}$. Adding another 18 studs, $m_p = 86$ in total, results in $N_{Ed,el} = 3422.6\,\text{kN} > N_{Ed}$ and guarantees that shear demand is greater than the desired 0.95. In fact, now the exact value of the shear demand can be computed through Eq. (38), cf. Table 2.

Adopting the stiffness method improves the shear demand, which is neglected in the strength method required by current design guides [1, 2]. Thus, the StiffM limits the ratio L_{nb} to H which ensures the composite column's ability to transfer longitudinal shear force resulting from bending or incipient buckling. In a considered case, the number of studs calculated directly from β_{min} read from the design chart results in a sufficient shear demand despite $N_{Ed} > N_{Ed,el}$. Adding another 18 studs does not improve the shear demand substantially (Fig. 13), yet it is rather a particularity for the given column. In general, the increase of studs to attain $N_{Ed,el} \geq N_{Ed}$ is recommended if one pursues fast design

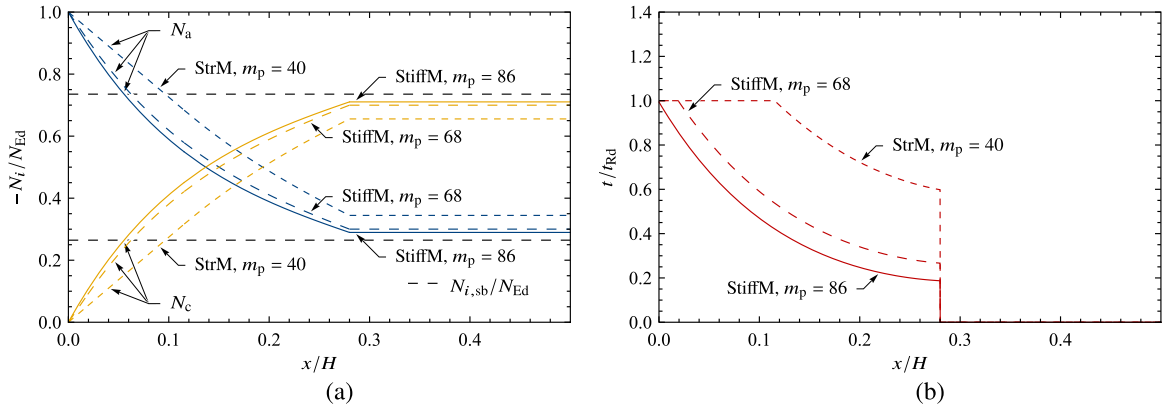

Fig. 13. Comparison of cross-sectional forces (a) and unit shear force $t(x)$ (b) for studs calculated with StrM, StiffM without ($N_{Ed} > N_{Ed,el}$), and with ($N_{Ed} < N_{Ed,el}$) adjusting the number of studs for the column loaded through steel.

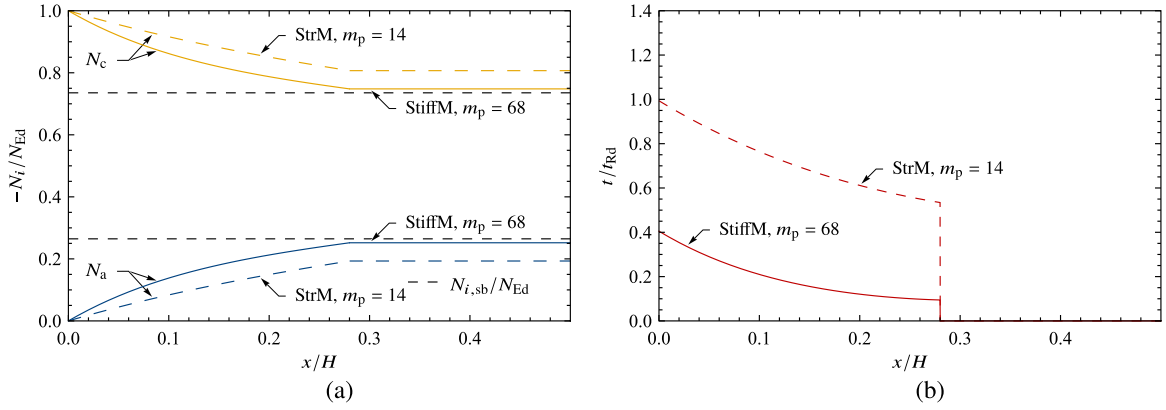

Fig. 14. Comparison of cross-sectional forces (a) and unit shear force $t(x)$ (b) for studs calculated with StrM and StiffM for the column loaded through concrete.

Table 2
Summary of attained shear demand κ and relative extent of the natural bond mobilization L_{nb}/H with StrM and StiffM.

Transfer	V_{Ed} [kN]	StrM			StiffM detailed ($N_{Ed} > N_{Ed,el}$)			StiffM fast ($N_{Ed} < N_{Ed,el}$)		
		m_p	κ	L_{nb}/H	m_p	κ_{ep}	L_{nb}/H	m_p	κ	L_{nb}/H
a → c	2500.3	40	0.891	0.19	68	0.952	0.08	86	0.966	0.06
c → a	899.7	14	0.730	0.17	–			68	0.952	0.03

instead of a more detailed and economical one which requires solving Eqs. (33) and (34).

For completeness, we provide the results of StrM and StiffM applied to the same composite column loaded through concrete by the same N_{Ed}. The design shear force V_{Ed} is much lower as the concrete part of the cross-section is the main bearer of the axial force (Table 2). Hence, the StrM produces only 14 studs and shear demand 0.730. Yet, the ratio L_{nb} to H is lower than in the loading through steel scenario because of the lesser V_{Ed}.

In addition, the StiffM results in exactly the same number of studs regardless of the load introduction direction for β_{min} read from the design chart. However in the case of loading through concrete, $m_p = 68$ results in $N_{Ed,el,c} = 8379.2\,kN > N_{Ed}$ and calculation stops. Yet without considering the extent of the natural bond mobilization, the same shear demand for much lower V_{Ed} produces limited utilization of the shear connection, cf. Fig. 14. The lower shear demand, e.g., $\kappa = 0.90$ would lead to a more economical design for the considered column, axial load, and loading direction.

The StiffM is especially useful for composite columns loaded through the cross-section part which is the main load bearer. As discussed extensively in Section 2, for typical columns where the buckling drives the maximal load, the axial stiffness is the key factor to establish the main load bearer. In the considered column the ratio $E_c A_c/(E_a A_a) = 1/(\alpha\omega) = 2.78$, hence for loading through concrete the design charts (Fig. 12) are readily applicable.

Also, note that the considerations presented assumed relatively weak studs: grade S235 and $h_{sc}/d_{sc} \approx 3.16$, cf. Eqs. (13) and (14). The disproportion between the results obtained with StrM and StiffM would be even more pronounced for studs with higher design resistance P_{Rd} and the same stiffness k_{sc} as is the case for $d_{sc} = 19\,mm$ where recommended by EN 1994-1-1 [1] $k_{sc} = 100\,kN/mm$, regardless of the studs grade and proportions. Moreover, the range of applicability of the design charts would be wider as $N_{Ed,el}$ depends linearly on the ratio $t_{Rd}/k = P_{Rd}/k_{sc}$ for given load introduction length L_t, cf. Eqs. (32) and (42).

6. Conclusions

The key takeaways from the presented study are as follows:

1. The stiffness-based force allocation (2) is more adequate than the capacity-based force allocation (1) for the axial loads typically arising in the design of composite columns.
2. For the considered load levels ($n \leq 0.4$), the results from the stiffness-based force allocation differed from the actual force distribution concerning the nonlinear model of concrete [1] no

more than 5%, while the discrepancy between the capacity-based force allocation and the actual force distribution, in some cases, might reach 35%.
3. The stiffness of the shear connection in the load introduction area is essential to properly transfer the shear force between the cross-section parts, which has not received a due consideration to date.
4. We have proposed a new Stiffness Method, which aims to ensure the effective transfer of shear and thus limit the extent of the natural bond mobilization outside the load introduction area.
5. Design charts for four levels of the shear demand has been provided and applied to the design example, which has shown the difference between the proposed Stiffness and currently adopted in standards [1,2] Strength Methods.

CRediT authorship contribution statement

B. Grzeszykowski: Conceptualization, Methodology, Software, Validation, Writing – original draft. **M.J. Lewandowski-Szewczyk:** Methodology, Software, Validation, Visualization, Writing – review & editing. **M. Niedośpiał:** Writing – review & editing.

Declaration of competing interest

The authors declare that they have no known competing financial interests or personal relationships that could have appeared to influence the work reported in this paper.

Data availability

Data will be made available on request.

References

[1] EN 1994-1-1. Eurocode 4: Design of composite steel and concrete structures — Part 1-1: General rules and rules for buildings. European standard, Brussels, Belgium: European Committee for Standardization; 2004.
[2] AISC 360-16. Specification for Structural Steel Buildings. An American National Standard, Chicago, IL: American Institute of Steel Construction; 2016.
[3] Wium JA, Lebet J-P. Simplified calculation method for force transfer in composite columns. J Struct Eng 1994;120:728–46. http://dx.doi.org/10.1061/(ASCE)0733-9445(1994)120:3(728.
[4] Johnson RP. Designers' Guide to Eurocode 4: Design of Composite Steel and Concrete Structures: EN 1994-1-1. 2nd ed. London, UK: ICE Publishing; 2012.
[5] EN 1992-1-1. Eurocode 2: Design of concrete structures — Part 1-1: General rules and rules for buildings. European standard, Brussels, Belgium: European Committee for Standardization; 2004.
[6] EN 1993-1-1. Eurocode 3: Design of steel structures — Part 1-1: General rules and rules for buildings. European standard, Brussels, Belgium: European Committee for Standardization; 2005.
[7] Viest IM. Investigation of stud shear connectors for composite concrete and steel T-beams. In: J Proc Vol. 52. 1956, p. 875–92. http://dx.doi.org/10.14359/11655.
[8] Xue W, Ding M, Wang H, Luo Z. Static Behavior and Theoretical Model of Stud Shear Connectors. J Bridge Eng 2008;13:623–34. http://dx.doi.org/10.1061/(ASCE)1084-0702(2008)13:6(623).
[9] Xue D, Liu Y, Yu Z, He J. Static behavior of multi-stud shear connectors for steel-concrete composite bridge. J Construct Steel Res 2012;74:1–7. http://dx.doi.org/10.1016/j.jcsr.2011.09.017.
[10] Roeder CW. Bond Stress of Embedded Steel Shapes in Concrete. In: Effects of Damage and Redundancy on Structural Performance. New York, NY: American Society of Civil Engineers; 1985, p. 227–40.
[11] Hunaiti YM. Bond Strength in Battened Composite Columns. J Struct Eng 1991;117:699–714. http://dx.doi.org/10.1061/(ASCE)0733-9445(1991)117:3(699).
[12] Roeder CW, Cameron B, Brown CB. Composite Action in Concrete Filled Tubes. J Struct Eng 1999;125:477–84. http://dx.doi.org/10.1061/(ASCE)0733-9445(1999)125:5(477).
[13] Grzeszykowski B, Szadkowska M, Szmigiera E. Analysis of Stress in Steel and Concrete in CFST Push-Out Test Samples. Civ Environ Eng Rep 2017;145–59. http://dx.doi.org/10.1515/ceer-2017-0042.
[14] Dunberry E, Leblanc D, Redwood RG. Cross-section strength of concrete-filled HSS columns at simple beam connections. Can J Civil Eng 1987;14:408–17. http://dx.doi.org/10.1139/l87-059.
[15] Mollazadeh MH, Wang YC. New insights into the mechanism of load introduction into concrete-filled steel tubular column through shear connection. Eng Struct 2014;75:139–51. http://dx.doi.org/10.1016/j.engstruct.2014.06.002.
[16] Mollazadeh MH, Wang YC. New Mechanism of Load Introduction into Concrete-Filled Steel Tubular Columns. J Struct Eng 2016;142:04016016. http://dx.doi.org/10.1061/(ASCE)ST.1943-541X.0001470.
[17] Wium JA. Composite columns: Force transfer from steel section to concrete encasement (Ph.D. thesis), Lausanne, Switzerland: École Polytechnique Fédérale de Lausanne; 1992, http://dx.doi.org/10.5075/epfl-thesis-1008.
[18] Hegemier GA, Murakami H, Hageman LJ. On tension stiffening in reinforced concrete. Mech Mater 1985;4:161–79. http://dx.doi.org/10.1016/0167-6636(85)90014-6.
[19] Walraven J, Bigaj-van Vliet A, editors. Fib Model Code for Concrete Structures 2010. Berlin, Germany: Ernst & Sohn; 2013.
[20] Marti P, Alvarez M, Kaufmann W, Sigrist V. Tension Chord Model for Structural Concrete. Struct Eng Int 1998;8:287–98. http://dx.doi.org/10.2749/101686698780488875.
[21] Johansson M, Gylltoft K. Mechanical Behavior of Circular Steel-Concrete Composite Stub Columns. J Struct Eng 2002;128:1073–81. http://dx.doi.org/10.1061/(ASCE)0733-9445(2002)128:8(1073).
[22] Popovics S. A numerical approach to the complete stress–strain curve of concrete. Cem Concr Res 1973;3:583–99. http://dx.doi.org/10.1016/0008-8846(73)90096-3.
[23] Tsai WT. Uniaxial Compressional Stress-Strain Relation of Concrete. J Struct Eng 1988;114:2133–6. http://dx.doi.org/10.1061/(ASCE)0733-9445(1988)114:9(2133).
[24] Mander JB, Priestley MJN, Park R. Theoretical Stress-Strain Model for Confined Concrete. J Struct Eng 1988;114:1804–26. http://dx.doi.org/10.1061/(ASCE)0733-9445(1988)114:8(1804.
[25] Tao Z, Wang Z-B, Yu Q. Finite element modelling of concrete-filled steel stub columns under axial compression. J Construct Steel Res 2013;89:121–31. http://dx.doi.org/10.1016/j.jcsr.2013.07.001.
[26] Kwon S-H, Kim T-H, Kim Y-Y, Kim J-K. Long-term behaviour of square concrete-filled steel tubular columns under axial service loads. Mag Concr Res 2007;59:53–68. http://dx.doi.org/10.1680/macr.2007.59.1.53.
[27] Wang X, Liu Y, Li Y, Lu Y, Li X. Bond behavior and shear transfer of steel section–concrete interface with studs: Testing and modeling. Constr Build Mater 2020;264:120251. http://dx.doi.org/10.1016/j.conbuildmat.2020.120251.
[28] Grzeszykowski B, Szmigiera E. Nonlinear longitudinal shear distribution in steel-concrete composite beams. Arch Civ Eng 2019;65:65–82. http://dx.doi.org/10.2478/ace-2019-0005.
[29] Oehlers DJ, Coughlan CG. The shear stiffness of stud shear connections in composite beams. J Construct Steel Res 1986;6:273–84. http://dx.doi.org/10.1016/0143-974X(86)90008-8.
[30] Shim C-S, Lee P-G, Yoon T-Y. Static behavior of large stud shear connectors. Eng Struct 2004;26:1853–60. http://dx.doi.org/10.1016/j.engstruct.2004.07.011.
[31] Meng H, Wang W, Xu R. Analytical model for the Load-Slip behavior of headed stud shear connectors. Eng Struct 2022;252:113631. http://dx.doi.org/10.1016/j.engstruct.2021.113631.
[32] Salari MR, Spacone E, Shing PB, Frangopol DM. Nonlinear Analysis of Composite Beams with Deformable Shear Connectors. J Struct Eng 1998;124:1148–58. http://dx.doi.org/10.1061/(ASCE)0733-9445(1998)124:10(1148).
[33] Zona A, Ranzi G. Shear connection slip demand in composite steel-concrete beams with solid slabs. J Construct Steel Res 2014;102:266–81. http://dx.doi.org/10.1016/j.jcsr.2014.07.018.
[34] Buru SM, Chiorean CG, Botez M. Elastic Analysis of Steel-Concrete Composite Beams with Partial Interaction. IOP Conf Ser: Mater Sci Eng 2021;1203:032110. http://dx.doi.org/10.1088/1757-899X/1203/3/032110.
[35] Khan AS, Huang S. Continuum Theory of Plasticity. New York, USA: John Wiley & Sons; 1995.
[36] Prakash A, Anandavalli N, Madheswaran CK, Lakshmanan N. Modified Push-out Tests for Determining Shear Strength and Stiffness of HSS Stud Connector-Experimental Study. Int J Comput Mater 2012;2:22–31. http://dx.doi.org/10.5923/j.cmaterials.20120203.02.
[37] He J, Lin Z, Liu Y, Xu X, Xin H, Wang S. Shear stiffness of headed studs on structural behaviors of steel-concrete composite girders. Steel Compos Struct 2020;36:553–68. http://dx.doi.org/10.12989/scs.2020.36.5.553.
[38] Wang C, Cao D, Liu X, Jing Y, Liu W, Yang G. Initial Elastic Stiffness of Bolted Shear Connectors in Steel-Concrete Composite Structures. Adv Civ Eng 2022;7008727. http://dx.doi.org/10.1155/2022/7008727.
[39] Grzeszykowski B, Szmigiera ED. Analysis of the load transfer between materials in composite concrete encased steel columns loaded axially. ce/papers 2017;1:2090–9. http://dx.doi.org/10.1002/cepa.254.

[40] Korelc J. Multi-language and Multi-environment Generation of Nonlinear Finite Element Codes. Eng Comput 2002;18:312–27. http://dx.doi.org/10.1007/s003660200028.
[41] Alart P, Curnier A. A mixed formulation for frictional contact problems prone to Newton like solution methods. Comput Methods Appl Mech Engrg 1991;92:353–75. http://dx.doi.org/10.1016/0045-7825(91)90022-x.
[42] Lengiewicz J, Korelc J, Stupkiewicz S. Automation of finite element formulations for large deformation contact problems. Internat J Numer Methods Engrg 2011;85:1252–79. http://dx.doi.org/10.1002/nme.3009.
[43] Lewandowski-Szewczyk MJ, Stupkiewicz S. Non-standard contact conditions in generalized continua: microblock contact model for a Cosserat body. Int J Solids Struct 2020;202:881–94. http://dx.doi.org/10.1016/j.ijsolstr.2020.07.001.